

## Experiment Report Form

**The double page inside this form is to be filled in by all users or groups of users who have had access to beam time for measurements at the ESRF.**

Once completed, the report should be submitted electronically to the User Office via the User Portal:

<https://www.esrf.fr/misapps/SMISWebClient/protected/welcome.do>

### ***Reports supporting requests for additional beam time***

Reports can be submitted independently of new proposals – it is necessary simply to indicate the number of the report(s) supporting a new proposal on the proposal form.

The Review Committees reserve the right to reject new proposals from groups who have not reported on the use of beam time allocated previously.

### ***Reports on experiments relating to long term projects***

Proposers awarded beam time for a long term project are required to submit an interim report at the end of each year, irrespective of the number of shifts of beam time they have used.

### ***Published papers***

All users must give proper credit to ESRF staff members and proper mention to ESRF facilities which were essential for the results described in any ensuing publication. Further, they are obliged to send to the Joint ESRF/ ILL library the complete reference and the abstract of all papers appearing in print, and resulting from the use of the ESRF.

Should you wish to make more general comments on the experiment, please note them on the User Evaluation Form, and send both the Report and the Evaluation Form to the User Office.

### **Deadlines for submission of Experimental Reports**

- 1st March for experiments carried out up until June of the previous year;
- 1st September for experiments carried out up until January of the same year.

### **Instructions for preparing your Report**

- fill in a separate form for each project or series of measurements.
- type your report, in English.
- include the reference number of the proposal to which the report refers.
- make sure that the text, tables and figures fit into the space available.
- if your work is published or is in press, you may prefer to paste in the abstract, and add full reference details. If the abstract is in a language other than English, please include an English translation.



	<b>Experiment title:</b> <b>Structural dynamics of laser excited lipid membranes</b>	<b>Experiment number:</b> SC3150
<b>Beamline:</b> ID09B	<b>Date of experiment:</b> from: 08.05.2011 to: 14.05.2011	<b>Date of report:</b> 31.08.2011
<b>Shifts:</b> 15	<b>Local contact(s):</b> M. Wulff, D Khakhulin	<i>Received at ESRF:</i>
<b>Names and affiliations of applicants (* indicates experimentalists):</b> T. Reusch* <sup>1</sup> , D.-D. Mai* <sup>1</sup> , J. Hallmann* <sup>1</sup> , T. Salditt* <sup>1</sup> University of Göttingen, Institute for X-ray physics, 37077 Göttingen		

We report a time resolved scattering experiment on multilamellar lipid membranes over a broad range of time scales and under two conceptionally different ambient conditions. The structural dynamics after shot pulse excitation by the electric field of two different laser systems ( $\tau=1\text{ps}$ ,  $\lambda = 800\text{nm}$  and  $\tau=150\text{ns}$ ,  $\lambda = 532\text{nm}$ ) has been investigated in view of the non-equilibrium dynamics in lipid membranes. Physiological as well as technically relevant field regimes have been applied. The main experimental challenges here are related to (i) thermal drift and denaturing of the lipid membranes due to the pumping laser, (ii) drift induced by the synchrotron beam, and (iii) the up to date unknown nature / time scales of non equilibrium fluctuations in lipid membranes, as well as the dependence on the length of the pump pulse.

**Materials and Methods** – Highly oriented lipid multilamellar stacks of 1,2-Dioleoyl-*sn*-glycero-3-phosphatidylcholine (DOPC), 1,2-dioleoyl-*sn*-glycero-3-phospho-L-serine (DOPS) and 1,2-Diphytanoyl-*sn*-glycero-3-phosphatidylcholine (DPhPC) were deposited on solid substrates. Samples were mounted on a goniometer head (Huber) above the hphi (angle of incidence) rotation and illuminated under grazing incidence conditions. In a non-specular GISAXS geometry, one observes a set of diffuse 'Bragg sheets' along the  $q_z$ -axis. These Bragg-Sheets carry information about structural and elastic properties of the sample system. The diffuse scattering signals were recorded by a MarCCD detector 500mm behind the sample. In addition to the diffuse scattering patterns we recorded time resolved rocking curves in which a photodiode was used as a point detector. Both measurements have been performed using undulator radiation (U17) at an energy of 17keV at ID09B, the x-ray beamsizes on the sample was  $\sim 0,3 \cdot 0,15\text{mm}^2$  ( $h \cdot v$ ). In order to study / exclude thermal effects induced by a heating of the substrate due to the pumping laser we used two different types (polished Si-wafer and quartz glass) of substrates. In the case of silicon substrates we expected strong thermal effects for pumping wavelengths  $< 1300\text{nm}$ , whereas the glass substrate should be transparent throughout the achievable wavelength range. To reduce possible remaining hydration related artefacts to an absolute minimum, we kept our samples in direct contact with liquid water during parts of the experiment. In addition to the drift related advantages this allows for a controlled variation of osmotic stress and salt concentration. In the first part of the experiment we used the pico second laser system (Legend Elite, Coherent) available at the ID09B for optical pumping. At a quasi parallel excitation geometry ( $\alpha_i \sim 10^\circ$ ), the sample was placed in the defocus of a planoconvex lens, resulting in a laser beam size of  $\sim 1 \cdot 1\text{mm}^2$  at the sample position. Laser polarization could be controlled with a  $\lambda/2$  plate in front of the focussing lens. In the second part of the experiment we used the nanosecond laser system ( $\tau=150\text{ns}$ ,  $\lambda = 532\text{nm}$ ) for optical excitation. Beam steering and optical alignment were identical to the case of pico second pumping, the  $10^5$  increase in pulse duration however leads to dramatically decreased peak intensities and field strengths. Signal- (pumped) and drift ( $-10\mu\text{s}$  reference) diffraction patterns have been measured in an alternating manner. Due to this measurement protocol, every

second diffraction pattern is effectively un-pumped and can be used in order to monitor drift effects. Hence it will be referred to as 'drift measurement' throughout the following report.

**Results (picosecond pumping) :** The first part of the experiment was devoted to the elimination of laser- as well as x-ray induced drift. The diffuse scattering patterns have been dark corrected, normalized to the storage ring current and symmetrized before the integrated intensity, FWHM ( $q_z$  as well as  $q_r$ ) and the center of mass of each reflection has been analysed. For samples hydrated by water vapour, drift induced by x-rays (possibly due to charging) as well as laser radiation (by heat induced changes in local rel.humidity) has been found to be the dominant effect in all cases. This drift is characterized by a shrinking of the bilayer periodicity in response to laser and expansion in response to x-ray exposure. Note that these opposite effects can be tricky to disentangle ! The shrinking continues seamlessly for repetitive measurements (figure 1.b) and saturates after thermal equilibrium has been reached. After significant experimental work (checked for wavelength- and substrate dependence ...) these drift effects could be successfully eliminated (x-ray induced) and minimized (laser induced) by keeping the samples in contact with liquid water in a dedicated sample chamber during the experiment. Laser induced drift can in this case be characterized by a slight shrinking of the lipid membrane (figure 1.b), x-ray induced drift was finally absent in the measurements. For a picosecond laser excitation, no field induced reversible dynamics was detectable up to the destruction threshold of the sample. At laser pump pulse intensities  $>10^{10} \text{W/cm}^2$ , irreversible damage occurred.

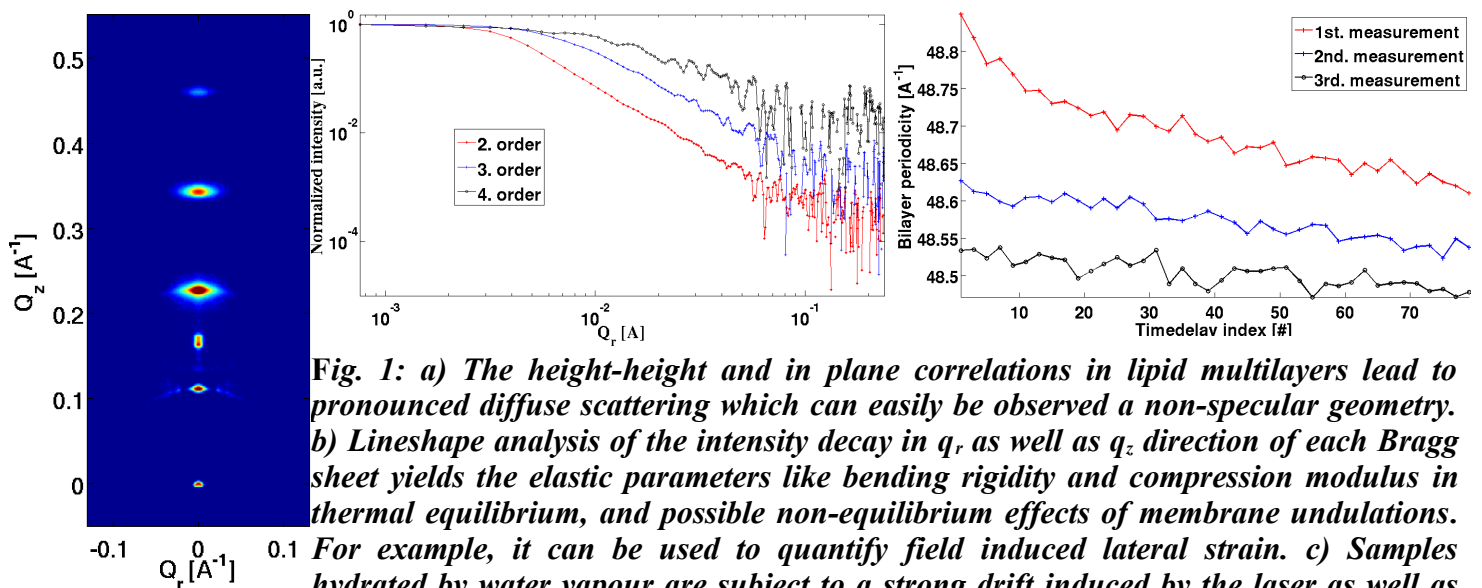


**Fig. 1:** a) The height-height and in plane correlations in lipid multilayers lead to pronounced diffuse scattering which can easily be observed a non-specular geometry. b) Lineshape analysis of the intensity decay in  $q_r$  as well as  $q_z$  direction of each Bragg sheet yields the elastic parameters like bending rigidity and compression modulus in thermal equilibrium, and possible non-equilibrium effects of membrane undulations.

For example, it can be used to quantify field induced lateral strain. c) Samples hydrated by water vapour are subject to a strong drift induced by the laser as well as the x-ray beam. The bilayer periodicity has been plotted as a function of acquisition number for three consecutive time resolved measurements. Time zero corresponds to acquisition number 30, pump intensity has been  $6 \cdot 10^8 \text{ W/cm}^2$  (@ one picosecond) .

**Results (nanosecond pumping) :** In order to overcome the 'quenched' nature of the sample system on fast timescales we switched to a nanosecond lasersystem ( $\tau=150\text{ns}$ ,  $\lambda = 532\text{nm}$ ) for the second part of the experiment. To minimize hydration related artefacts, the sample (in this case DPhPC) was kept in contact with a solution of Polyethylene Glycol (PEG) in water (MQ) at 30%wt. At pump intensities  $>0.5 \cdot 10^6 \text{W/cm}^2$  corresponding to an electric field  $E > 1,8 \cdot 10^6 \text{V/m}$  we were able to observe a characteristic increase in the amount of diffuse scattering, which is currently under quantitative analysis. Increasing the laser intensity above  $2 \cdot 10^6 \text{W/cm}^2$  resulted in an irreversible damage of our sample system. Because the remaining beamtime was rather limited we were not able to exploit this behaviour in further detail.

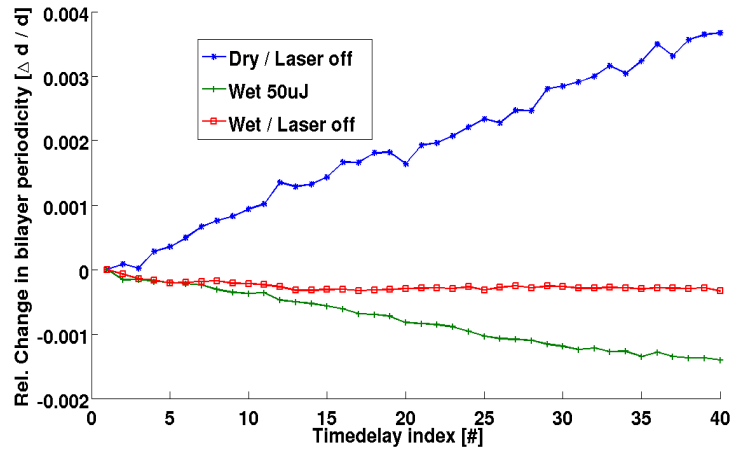
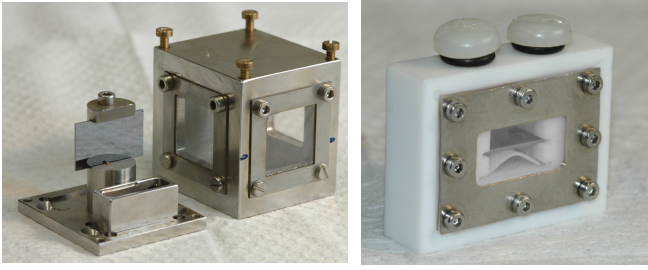


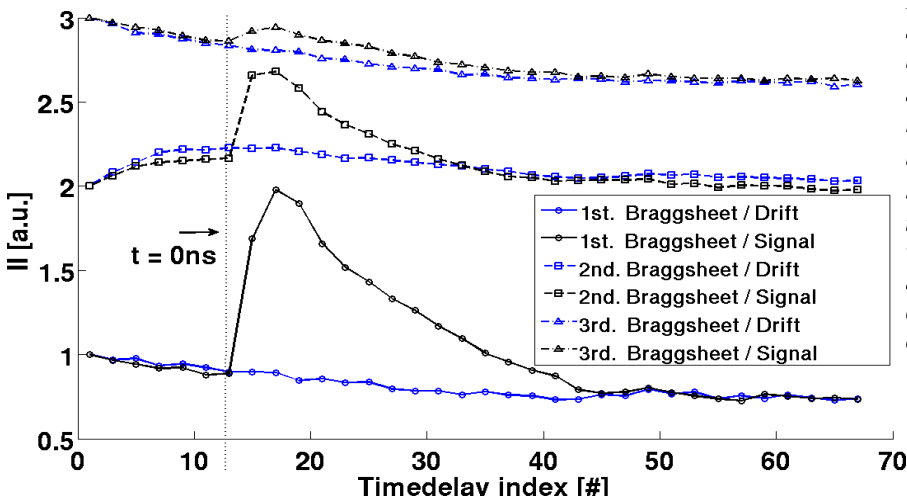
**Fig. 1:** Left: Sample cell used for time resolved scattering experiments on ('dry') lipid multilayers hydrated by water vapour. Relative ambient humidity can be adjusted by using saturated salt solutions, x-ray as well as laser radiation enters through 10 $\mu$ m thin mylar windows. Center: A precise variation of osmotic stress and salt concentration can be achieved in a dedicated ('wet') sample cell. The reservoir can be filled through inlets above the sample, absorption of laser radiation in liquid water is not mentionable at  $\lambda=800$ nm. Right: X-ray induced drift could be eliminated by keeping the sample in contact with liquid water during the experiment. Measurements have been normalized and plotted against acquisition number rather than time delay in order to avoid confusion due to the non equidistant spacing between individual delay values and to emphasize drift effects. Time zero corresponds to acquisition number 15, pump intensity has been  $6 \cdot 10^8$  W/cm $^2$  in case of the pumped (green, +) measurement.

n	$\Pi$ [a.u]	$\Delta \Pi_S$ [%]	$\Delta \Pi_D$ [%]	COM $^z$ [ $\text{\AA}^{-1}$ ]	$\Delta \text{COM}_S^z$ [%]	$\Delta \text{COM}_D^z$ [%]	FWHM $^x$ [ $\cdot 10^{-3} \cdot \text{\AA}^{-1}$ ]	$\Delta \text{FWHM}_S^x$ [%]	$\Delta \text{FWHM}_D^x$ [%]
1	$1.39 \cdot 10^3$	39.05	8.27	0.11	12.89	15.21	3.09	3.73	3.41
2	$9.97 \cdot 10^3$	17.61	5.87	0.23	15.58	18.47	4.51	3.33	3.86
3	$1.90 \cdot 10^3$	15.95	14.84	0.34	13.48	16.22	7.38	3.53	3.74
4	$4.42 \cdot 10^2$	11.59	11.49	0.46	7.01	8.16	—	—	—
SB	$1.01 \cdot 10^3$	3.32	2.81	0.17	81.91	83.86	2.98	7.17	7.16

n	FWHM $^z$ [ $\cdot 10^{-3} \cdot \text{\AA}^{-1}$ ]	$\Delta \text{FWHM}_S^z$ [%]	$\Delta \text{FWHM}_D^z$ [%]	$\nu$ [1/ $\text{\AA}^{-1}$ ]	$\Delta \nu_S$ [%]	$\Delta \nu_D$ [%]
1	1.59	5.38	5.40	—	—	—
2	2.27	11.65	11.59	2.23	2.74	1.00
3	3.65	20.30	22.15	1.79	3.51	2.60
4	3.88	24.23	32.67	1.39	19.12	20.74
SB	1.48	3.94	3.48	2.70	4.07	4.42

**Tab 1:** Integrated peak intensity ( $\Pi$ ), peak position (COM), peak width in  $q_r$  as well as  $q_z$  (FWHM $^x$ , FWHM $^z$ ) direction and the characteristic exponent of the intensity decay in  $q_r$  direction: mean values and standard variation of the corresponding signal ( $\Delta_S$ ) and drift; ( $\Delta_D$ ) measurements have been tabulated for each Bragg sheet ( $n=1-4$ ) as well as the specular reflected synchrotron beam (SB) (analysis ongoing). The  $\Pi$  curves exhibit a reversible excitation-relaxation effect, see Fig.3, while the other observables show approximately the same relative variation as the drift curves.



**Fig. 3:** left) For the 150ns pump pulse, a strong increase of the diffuse scattering intensity can be observed for all Bragg sheets on sub- $\mu$ s second time scale, but the relaxation rates to thermal equilibrium are in the range of  $\sim 3-5\mu$ s. Pump Intensity has been  $10^6$ W/cm $^2$  (@ 150ns,  $\lambda=532$ nm). For the pump pulse, a ps or a 150ns pump pulse was available. For ps pulse excitation, the system was quenched and no structural dynamics is observed (after correction of artifacts).